

**Support Action for Strengthening PAlesthine  
capabilities for seismic Risk Mitigation  
**SASPARM 2.0****

**Deliverable D.F.2**

**Validation report of the implemented methodology**





## Deliverable contributors

Institute for Advanced Study of Pavia

Iason Grigoratos

Ricardo Monteiro

Paola Ceresa

i

## Deliverable reviewers

European Centre for Training and Research in  
Earthquake Engineering

Barbara Borzi



## INDEX

Index.....	ii
Index of figures .....	iii
Index of tables.....	iv
1. Scope.....	1
2. Introduction.....	4
3. Validating the applicability of SP-BELA – extension to irregular RC FRAME buildings .....	6
3.1 Methodology .....	6
3.2 RC structural models .....	7
3.2.1 Type A building .....	7
3.2.2 Type B building .....	8
3.3 Modelling parameters.....	9
3.4 Record selection .....	10
3.5 Results .....	10
4. Concluding remarks .....	13
5. Bibliography.....	14



## INDEX OF FIGURES

Figure 1.1: Flowchart of SP-BELA for the derivation of vulnerability curves for RC buildings (Borzi et al., 2008a).....	2
Figure 3.1: Time history analyses results for the <i>Type A regular</i> model (introduced in Section 3.2.1): bilinear and 2 <sup>nd</sup> degree polynomial fitting. The corresponding pushover curve is also plotted for illustration purposes only. ....	7
Figure 3.2: Example of a real <i>Type A</i> building (left); <i>Type A</i> structural model (right).....	8
Figure 3.3: Example of the slab-frame configuration of the front side of a <i>Type B</i> building (left); <i>Type B</i> structural model: regular (centre), irregular (right). ....	8
Figure 3.4: Acceleration Response Spectra (5% damping) of selected records for <i>Type B regular</i> model applying the CMS approach.....	10
Figure 3.5: Bilinear fitting results for <i>Type A</i> (left) and <i>B</i> (right), <i>regular</i> and <i>irregular</i> models.....	11
Figure 3.6: 2 <sup>nd</sup> degree polynomial fitting results for <i>Type A</i> (left) and <i>B</i> (right), <i>regular</i> and <i>irregular</i> models. ....	11
Figure 3.7: Logarithmic fitting results for <i>Type A</i> (left) and <i>B</i> (right), <i>regular</i> and <i>irregular</i> models. ....	12



## INDEX OF TABLES

Table 3.1: Geometric properties and characteristics of the four models .....	9
Table 3.2: Yield displacement $\Delta_y$ and base shear at yield $V_{by}$ values from bilinear fitting .....	11
Table 3.3: Coefficients at different ductility levels.....	12



## 1. SCOPE

The WebGIS platform developed for this project allows to identify on the Nablus map the position of the buildings for which the collection forms were compiled by practitioners and citizens. These forms are described in deliverable D.B.2. Using the information collected with the forms it is possible to assign to each building one of the structural typologies that classify the as-built in Nablus, previously identified and described in deliverable D.B.1.

As described in deliverable D.F.1, the evaluation of the seismic vulnerability of Palestinian buildings in the city of Nablus has been conducted using SP-BELA (Simplified Pushover-Based Earthquake Loss Assessment; Borzi et al., 2008a; 2008b; 2008c; 2016). It is a mechanics-based method for the evaluation of the building capacity through the calculation of pushover curves conducted on statistically representative populations of regular buildings. One thousand building realizations based on one prototype plan configuration are generated through Monte Carlo simulations by varying the geometrical characteristics, together with the mechanical properties of the materials. Once the representative sample of a given type of structure is defined, SP-BELA carries out a simulated design for each building, which will then be subjected to simplified nonlinear static analysis. The final product is a bilinear pushover curve along the most vulnerable axis. For non-seismically designed buildings that axis is usually along the least flexible direction, where the stiffness and the seismic demand are higher. If the beams and the length of the bays are similar in both directions, the least flexible frame is the one with most spans. Furthermore, non-seismically designed buildings frequently have frames oriented in the longitudinal direction only. In the more flexible orthogonal direction, the frame effect is guaranteed by the floor slabs alone.

As a consequence of elastic perfectly plastic behaviour, only the base shear resistance collapse multiplier (based on the shear capacity of columns) and the displacement capacities (Priestley, 1997) need to be calculated to define the pushover curve. The fragility curves are generated comparing the displacement capacity identified on the pushover curve with the demand, defined from a displacement response spectrum. The principle behind the method is provided in Figure 1.1.

The present report aims at rendering the aforementioned procedure applicable to a larger population of buildings, thus improving the validity of the implemented methodology. Irregularities in plan and elevation are common in structures that do not comply with any building code; therefore SP-BELA should be adapted for these cases.

Borzi et al. (2008a, 2008c) have already tested the application of SP-BELA against regular RC frames. For irregular RC frame buildings however, the simplified-pushover based SP-BELA methodology cannot take into account the torsional modes. Such modes can play a role in RC buildings that very often have mass or stiffness irregularity in plan or elevation. This subject is analysed in the present deliverable. The report is focused on two irregular RC prototype buildings, representative of the common design practice in Palestine. The seismic assessment is carried out through *finite element model* (FEM) nonlinear time-history analyses, with a suitable set of scaled ground motion records that were selected using a recent state-of-the-art hazard model, specific for the Middle East region (EMME, 2013). The results were used to derive suitable building-class-specific correction factors.



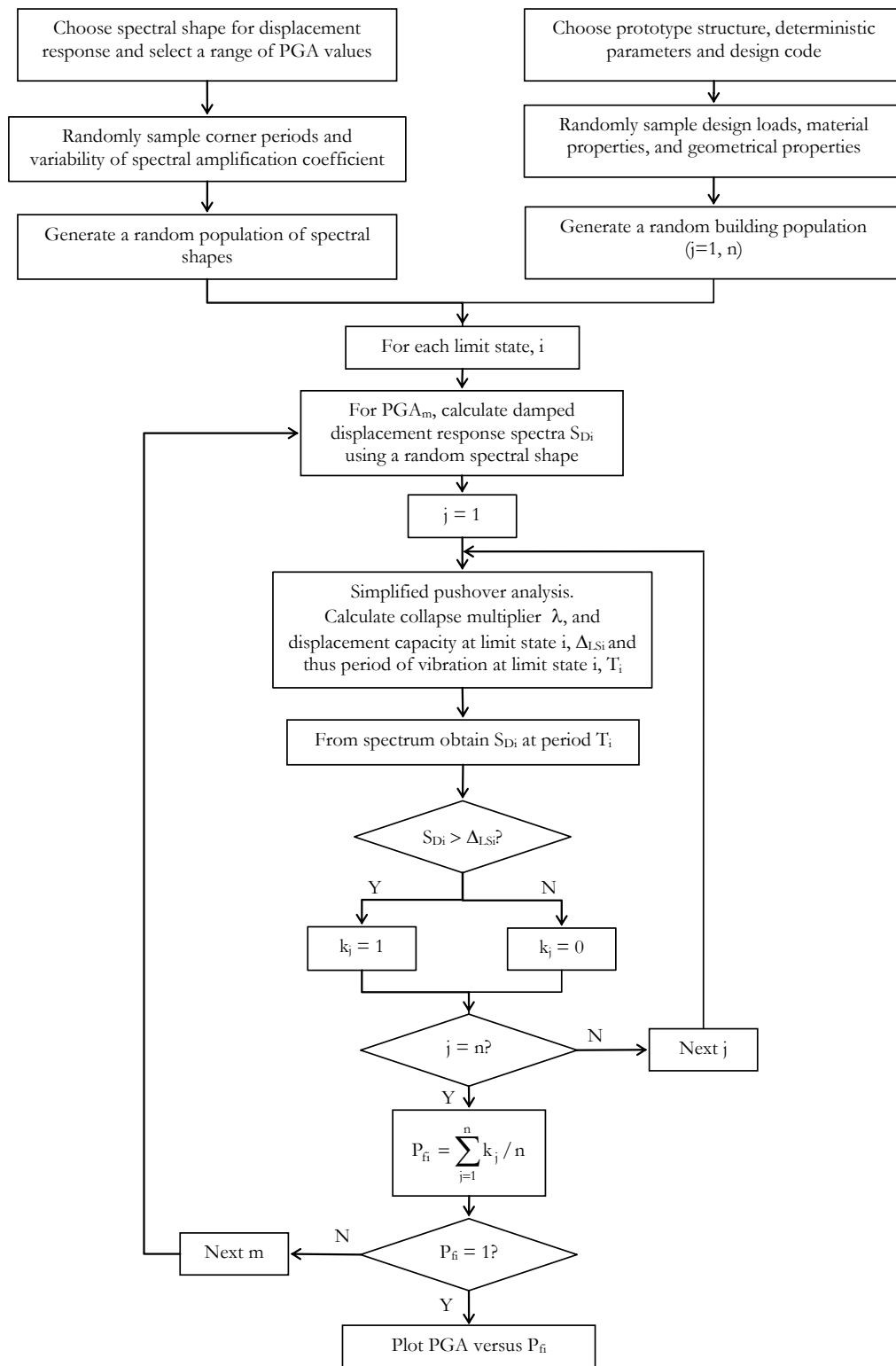


Figure 1.1: Flowchart of SP-BELA for the derivation of vulnerability curves for RC buildings (Borzi et al., 2008a).



As noted in deliverable D.F.1, regarding the RC buildings with shear walls, the definition of fragility curves for shear wall buildings has not been tackled through a mechanics-based methodology, since it is not possible to identify a prototype building which can be representative of the whole building stock. To address this problem, the fragility curves of shear wall buildings have been obtained from corresponding RC frame buildings. A coefficient has been calibrated in D.F.1 to identify the parameters of fragility curves for shear wall buildings starting from the curves of frame ones. This coefficient is based on the results of HAZUS (1999). Since the amount of buildings with shear walls is very limited and no prototype building can be attributed to this typology, no further validation has been conducted in the present report.

3

As far as the masonry buildings are concerned, SP-BELA has been already extended to this structural type in the past (Borzi et al., 2008b). Furthermore, the masonry buildings in Palestine usually have simple design in plan and no more than two stories. As such, no further investigation has been carried out in the present report.



## 2. INTRODUCTION

Fragility functions, representing the probability of exceeding a set of damage states conditional on a level of ground motion, are a fundamental component to describe the physical vulnerability of a population of buildings. They are useful for damage estimation, retrofitting decisions, loss estimation and disaster response planning.

There are only a few dozen places in the world where post-earthquake damage and repair cost data have been collected from a number of buildings large enough to permit the development of reliable empirical functions relating damage and repair cost data (Rossetto and Elnashai, 2003).

To overcome this limitation, analytical methodologies can be employed in either a single structure that is believed to be representative of a class of buildings, or a set of randomly generated buildings, modelled using structural analysis techniques, and subjected to specific lateral loading patterns or accelerograms. The simplest structural models employ equivalent single-degree-of-freedom (SDOF) systems. Although it is easy to obtain huge response statistics in a short period of time by using SDOF models (e.g. Silva et al., 2013), inspection of real structural response and damage distribution is not possible. The increase in the demand for reliable and more accurate loss estimations has triggered the development of fragility functions based on analytical/mechanical approaches which tend to provide a better representation of the structural behaviour of the building typologies. In many of the original procedures to define analytical vulnerability curves, nonlinear time-history analyses of prototype structures with randomly varying structural characteristics were carried out for a set of representative earthquakes (e.g. Singhal and Kiremidjian, 1996; Masi, 2004). However, running inelastic dynamic analyses for a large number of structures is extremely time consuming and alternative methods have thus been sought.

Inelastic static assessment approaches based on pushover analysis have been developed over the past two decades, such as the *N2 method* (Fajfar and Gaspersic, 1996) or the *Capacity Spectrum Method* (CSM; Freeman et al., 1975) among others. As described in Antoniou and Pinho (2004), they basically aim at identifying the structural performance by applying a response spectrum approach to a bilinear representation of an equivalent SDOF model derived from a pushover analysis of a multi-degree-of-freedom (MDOF) model of the structure under a force vector compatible with an assumed displacement profile. In the *N2 method*, an estimate of the seismic displacement demand is associated with the equal displacement rule, in the medium- and long-period ranges, employing inelastic spectra related to displacement-ductility demand. From the limit to displacement imposed by the calculated displacement demand, the structural performance quantities are extracted from the pushover analysis, hence local and global damage indices are determined. An improved version of this procedure (Fajfar, 2000) was incorporated in *Eurocode 8* (2004). On the other hand, particularly outside Europe, several research projects (e.g. HAZUS, 1999) have built upon the *Capacity Spectrum Method*. By means of a graphical procedure, the structural capacity and the seismic demand on the structure are overlapped. The capacity of the structure is represented converting the force-displacement curve, obtained by pushover analysis, to the so-called *ADRS capacity spectrum*, i.e. a plot of the accelerations and displacements of an equivalent SDOF system. A potential weakness is the difficulty in obtaining a physically realistic representation of the inelastic response of the structure using traditional pushover analysis. Many authors (e.g. Lawson et al., 1994; Chopra and Goel, 2006) have however noted that



inelastic static methods suffer from a series of limitations, which stem essentially from their inherently static nature. Such limitations become particularly evident in high-rise flexible frames (higher mode effects) and in buildings with mass or stiffness eccentricities (horizontal or vertical). As analysed in Pinho et al. (2013) and Monteiro et al. (2014), different methods have been proposed in an attempt to address this issue.

The *Adaptive Capacity Spectrum Method* (ACSM), proposed by Casarotti and Pinho (2007), uses displacement-based adaptive pushover analysis (Antoniou and Pinho 2004) to derive an equally adaptive SDOF capacity curve using the concept of substitute structure in *Acceleration Displacement* (AD) format, which is then used to derive the performance point by intersecting an appropriate over-damped elastic spectrum. *Modal Pushover Analysis* (MPA), as introduced by Chopra and Goel (2002), incorporates the effects of higher modes of vibration on structural responses and thus provides, in principle, improvement on the previously described procedures. In essence, this approach consists of employing a given nonlinear static procedure for each significant vibration mode of the structure and then carrying out an adequate combination of the modal structural responses. Kalkan and Kunnath (2006) proposed the *Adaptive Modal Combination* procedure (AMC), which accounts for higher-vibration-mode effects by combining the response of individual modal pushover analyses, which, however, incorporate the effects of progressive damage during the inelastic response. This procedure utilizes the energy-based formulation of equivalent SDOF systems to compute the dynamic performance point employing an inelastic response spectrum plotted method as well in AD format, and thus includes the graphical feature of the capacity spectrum.

Silva et al. (2014) note that although the above developments capture part of the problem, most of them are computationally significantly more expensive than the first generation of pushover methods.

*SASPARM 2.0* addresses this shortcoming with a building-class-specific approach, by extending the applicability of the simplified pushover-based seismic assessment model (SP-BELA) to irregular, yet common, structural configurations, that have been pre-identified based on field taxonomy data from the region in question. The idea is that the simplified bilinear pushover method is used for the regular (dominant translational first mode response) typologies whereas, for the irregular ones, a corresponding regular model is identified and analysed in order to define a coefficient that matches the regular building response to the irregular building one. In this way, the irregular distribution of stiffness or mass will be considered in a simplified - but yet acceptable for large-scale assessment studies - manner.



### 3. VALIDATING THE APPLICABILITY OF SP-BELA – EXTENSION TO IRREGULAR RC FRAME BUILDINGS

#### 3.1 Methodology

The present deliverable examines two irregular reinforced concrete (RC) prototype buildings, which are non-seismically designed and representative of the common construction practice in Nablus. The assessment of the structural performance of the prototype buildings is carried out through nonlinear time history analyses, with a suitable set of ground motion records that were selected using a recent state-of-the-art hazard model, specific for the Middle East region (EMME, 2013). For each irregular structure, a corresponding regular one, which the large-scale simplified pushover method is considered capable to assess, is defined. Besides the particular irregularity of each prototype, both the regular (R) and irregular (IR) versions have the same mean values (Table 3.1) of the distributions that define the geometric configurations and material properties of the building population (Borzi et al., 2016). For both versions of each prototype building, a set of case-specific records has been employed. The records were scaled at different levels, in order to run several one directional time-history analyses and get the maximum roof displacement  $\Delta$  and the maximum base shear  $V_b$ . Furthermore, the columns of the first floor were checked for yielding (*Eurocode 8* formulae). The elastic-range points and the inelastic-range points have been grouped separately and linear regression analysis has been applied to fit a bilinear pushover curve in order to define the yield displacement  $\Delta_y$  and corresponding base shear  $V_{by}$  (Figure 3.1). To get the mean capacity curve of the time history analyses all the points have been fitted with three different curves; bilinear, 2<sup>nd</sup> degree polynomial and logarithmic.

Afterwards, for each case, for different global ductility values  $\mu$ , the corresponding roof displacement  $\Delta$  and equivalent period  $T_{eq}$  have been computed according to Equations (3.1) to (3.3) (SI units).

$$T_{eq} = T_y \sqrt{\mu} \quad (3.1)$$

$$T_y = 2\pi \sqrt{\frac{M}{K_y}} \quad (3.2)$$

$$K_y = V_{by} / \delta_y \quad (3.3)$$

$M$  is the total mass of the building whilst the equivalent viscous damping  $\xi_{eq}$  in the inelastic range has been calculated according to Equation (3.4) by Priestley et al. (2007).

$$\xi_{eq} = 0.565 \frac{\mu - 1}{\pi \mu} \quad (3.4)$$

The corresponding spectral reduction factor  $\eta$  according to Bommer et al. (2000) and *Eurocode 8*, is given by Equation (3.5) and was applied to the displacement spectrum of Nablus coming from the local hazard model (EMME, 2013) in order to get the spectral displacement  $S_d(T_{eq})$ .

$$\eta = \sqrt{\frac{10}{5 + \xi_{eq}}} \quad (3.5)$$



The spectrum is calculated assuming a  $V_{s30}$  value of 800m/s (rock site conditions), which is the most common case in Nablus. The suitable correction factor for the simplified procedure is then defined according to Equation (3.6), where  $\Delta_{capacity}$  is the roof displacement of the corresponding ductility level, coming from the three possible fitting capacity curves.

$$\frac{\Delta_{capacity\_R}}{S_d(T_R) \eta_R} / \frac{\Delta_{capacity\_IR}}{S_d(T_{IR}) \eta_{IR}} \tag{3.6}$$

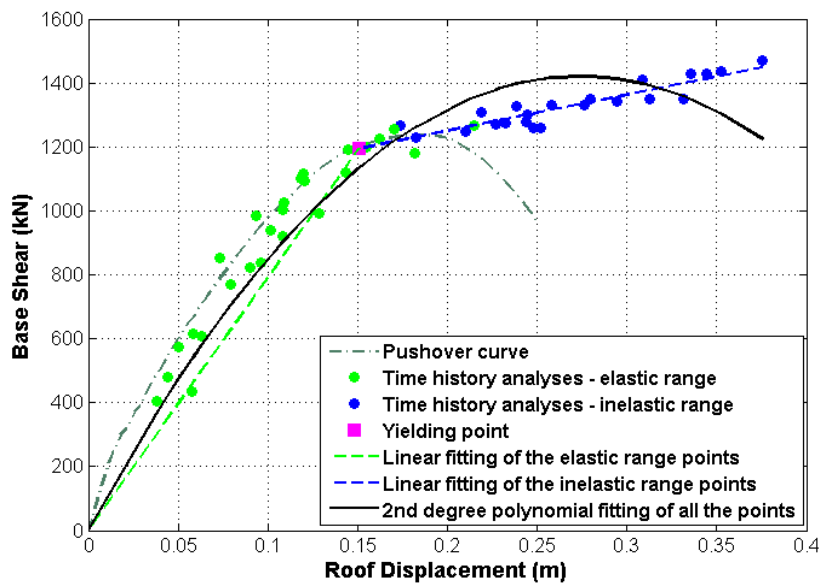


Figure 3.1: Time history analyses results for the *Type A regular* model (introduced in Section 3.2.1): bilinear and 2<sup>nd</sup> degree polynomial fitting. The corresponding pushover curve is also plotted for illustration purposes only.

### 3.2 RC structural models

The *SASPARM 2.0* project created a web database with vulnerability data on buildings in Nablus. Citizens, practitioners and students were involved in the in-situ collection through specific forms, which aimed at detecting the structural characteristics of Palestinian buildings (D.B.2, D.B.3, Monteiro et al, 2016). The forms allow a quick first screening of the building stock, since they include typological and metric data of the structures (Grigoratos et al., 2016). Almost all buildings in Nablus have not been designed to resist lateral loads. The *SASPARM 2.0* data allowed the identification of the two most common building typologies with torsional configuration in the city of Nablus, named, in the following, *Type A* and *Type B*.

#### 3.2.1 Type A building

This first type of building, illustrated in Figure 3.2, is characterized by a length ratio between the two principal axes of the building of 7 to 1, leading to torsional effects in the building response.





Figure 3.2: Example of a real *Type A* building (left); *Type A* structural model (right).

While validating SP-BELA, Borzi et al. (2008a) observed that the direction in which the mechanism of collapse is activated first, is almost always the direction where a frame effect is most evident. Therefore, the seismic input was applied in the longitudinal direction only. In order to induce a torsional response under unidirectional motion, in the irregular version only, a non-uniform distribution of the dead load was considered (i.e. a distribution of 55% and 45% of the dead load on the right and left set of longitudinal beams respectively). This modification proved to lead the irregular building to 3 to 15 times larger maximum torsional rotation in the columns.

### 3.2.2 *Type B* building

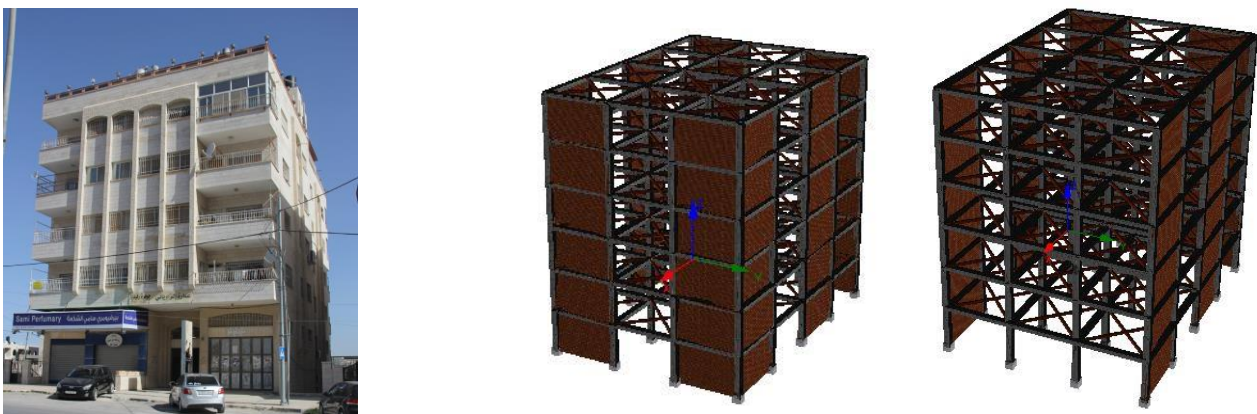


Figure 3.3: Example of the slab-frame configuration of the front side of a *Type B* building (left); *Type B* structural model: regular (centre), irregular (right).

Many residential buildings in Nablus have commercial stores at the first floor, which in favour of parking space lead the column frame two meters further back from the facade. The upper residential storeys have cantilever slabs above this offset. The heavy exterior infills in the front side of the upper storeys are, as a result, not aligned with the column frame and do not contribute to the total stiffness and are taken into account only as additional mass. This results in a stiffness irregularity in plan (irregular version, Figure 3.3-right). The equivalent model that SP-BELA could capture does not present this irregularity (regular version, Figure 3.3-centre). Furthermore, usually not all perimeter

bays have continuous infill panels, due to the presence of windows. That is the reason why the solid infill panels were included, at all floors, only in every other bay.

All building cases have mean concrete compressive strength of 28MPa, steel reinforcement strength of 420MPa, dead loads of 9.5kN/m<sup>2</sup>, square columns 450mm×450mm (4Φ18, Φ8/300, in mm) and wide short beams 300mm×500mm (4Φ14, Φ8/300, in mm). The values are representative of the in-built in Nablus (Grigoratos et al., 2016). The columns have been designed so that they undertake effective axial load  $\nu$  of around 0.4.

Table 3.1: Geometric properties and characteristics of the four models

	Type A		Type B	
	Regular	Irregular	Regular	Irregular
<i>Number of floors</i>	7	7	6	6
<i>Bay length</i>	5m	5m	5m	5m
<i>Bays in x axis</i>	7	7	4	4
<i>Bays in y axis</i>	1	1	3	3
<i>Height of 1st floor</i>	6m	6m	3.25m	3.25m
<i>Height of upper floors</i>	3.25m	3.25m	3.25m	3.25m
<i>Ground motion</i>	X axis only	X axis only	Y axis only	Y axis only
<i>Fundamental Period T<sub>1</sub></i>	2.1s	2.2s	0.8s	1.1s
<i>Disaggregation: Mean M<sub>w</sub>; R<sub>jb</sub>; ε</i>	6.82; 33.8km; 1.42		6.52; 25.2km; 1.46	
<i>Total mass (tons)</i>	2545	2545	3087	3010

### 3.3 Modelling parameters

The analyses have been carried out using the fibre-element software SeismoStruct (2014) and P-delta effects were taken into account. The diaphragm action has been modelled using horizontal elastic cylindrical X-braces (25cm diameter, 200GPa elastic modulus). In Nablus, around the elevator cores there is usually concrete U-shaped shear walls with poor reinforcement and no boundary elements (dummy columns). Furthermore, the aforementioned shear walls have weak corner connections and their exact location cannot be correlated with the rest of the Monte Carlo sampling variables. For this reason, they were not included in the SP-BELA model nor in this study’s finite element models, although they could introduce further torsional response if they were non-symmetrically placed and had more rigid corner connections.

The exterior infill walls in Nablus usually consist of hollow concrete blocks (100mm), weak unreinforced concrete layer (130mm, around 12MPa mean compressive strength) and stone layer of about 70mm. Their weight is around 4.75kN/m<sup>2</sup>. Due to lack of experimental data for this multi-layer configuration, it was decided to model only the strongest middle layer using the model by Crisafulli (1997) which is incorporated in the software. The elastic modulus was taken as 6.5GPa (cracked section), while the strut area was 0.057m<sup>2</sup>.



### 3.4 Record selection

In 2013, a project with the purpose of contributing to seismic risk reduction in the Middle East developed an updated Earthquake Model of the Middle East Region (EMME, 2013), seeking a uniform calculation of the regional seismic hazard. This has been further employed to select natural records for this study. A disaggregation analysis has been conducted for Nablus city using OpenQuake (Pagani et al., 2014). The dominant focal mechanism (strike slip) and the mean magnitude  $M_w$ , Joyner-Boore distance  $R_{jb}$ , epsilon  $\epsilon$  values indicated in Table 3.1 were used together with the fundamental elastic period of the structure, as input for the *Conditional Mean Spectrum* approach (CMS; Baker, 2010; Jayaram et al., 2011) – Figure 3.4. The *Ground Motion Prediction Equation* developed by Chiou and Youngs (2008), the one with the largest weight in EMME’s logic tree, was used. Three different sets of 10 records have been extracted, given that *Type A irregular* has almost the same period as the regular. The 5%-95% *effective duration* (Trifunac and Brady, 1975) of the records was considered.

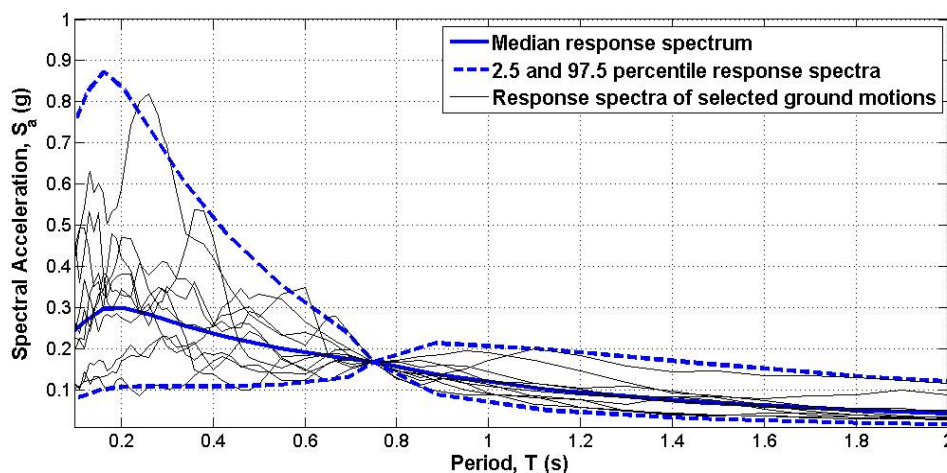


Figure 3.4: Acceleration Response Spectra (5% damping) of selected records for *Type B regular* model applying the CMS approach.

### 3.5 Results

SP-BELA checks the shear capacity of the columns according to *Eurocode 2* (2004), assuming a strut angle of  $45^\circ$ . Since the columns have been dimensioned so that they undertake effective axial load “ $\nu$ ” of around 0.4, even though the transverse reinforcement is quite scarce, no early shear failures were observed. SP-BELA assumes that gravity load design typically features high shear forces in the beams and thus these elements have traditionally been provided with an adequate amount of shear reinforcement. Therefore, the methodology takes only the flexural collapse mechanism into account for the beams. All buildings present a column-sway plastic mechanism. The roof yield displacement and base shear at yield, calculated based on the refined bilinear fitting of the time history results (Figure 3.1), are presented in





Table 3.2

Table 3.2: Yield displacement  $\Delta_y$  and base shear at yield  $V_{by}$  values from bilinear fitting.

	Type A		Type B	
	Regular	Irregular	Regular	Irregular
Yield Displacement $\Delta_y$ (m)	0.150	0.130	0.101	0.074
Base shear at yield $V_{by}$ (kN)	1178	1142	6264	4515

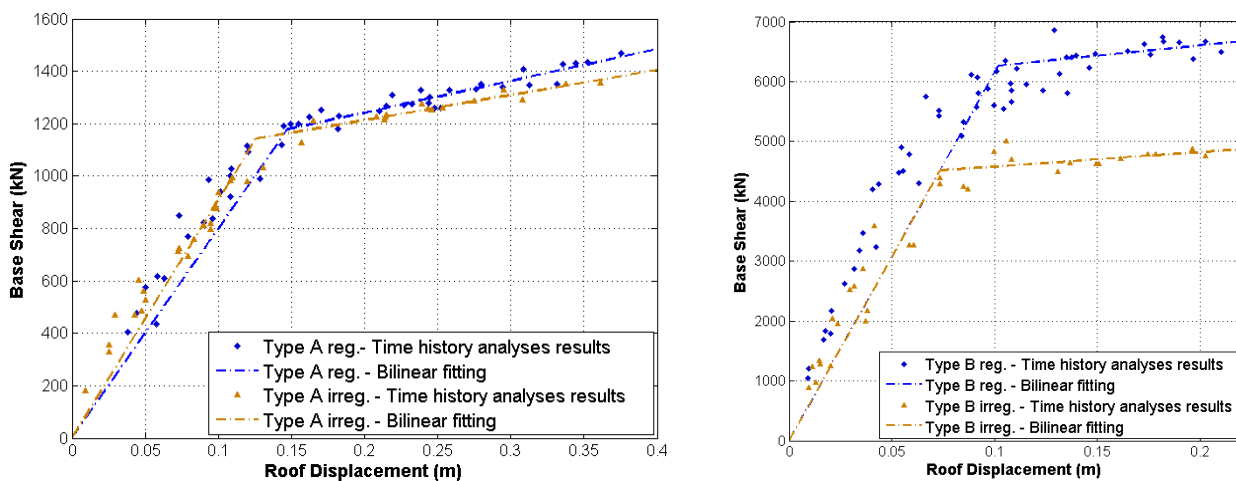


Figure 3.5: Bilinear fitting results for Type A (left) and B (right), regular and irregular models.



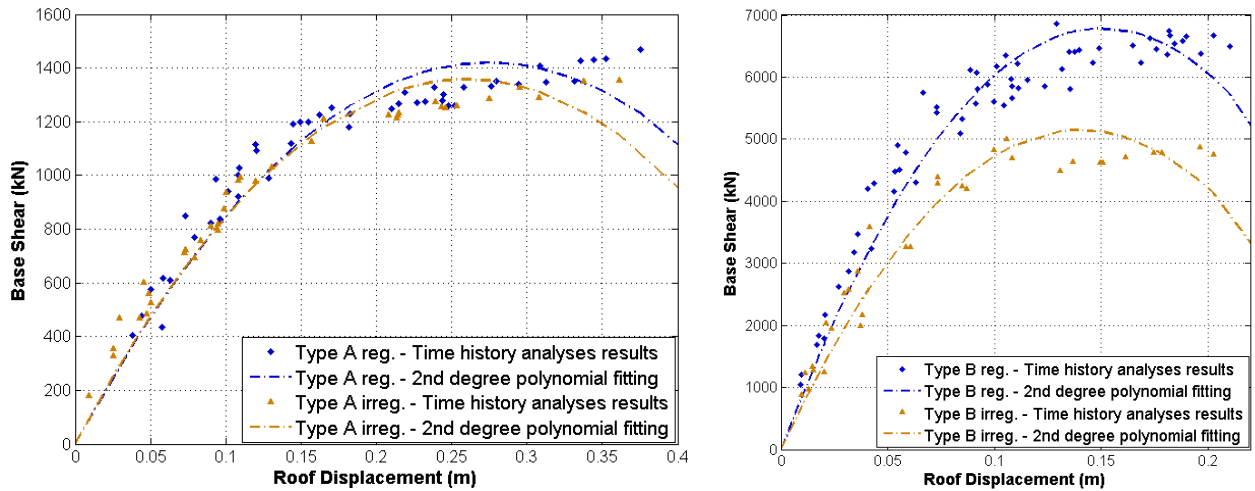


Figure 3.6: 2<sup>nd</sup> degree polynomial fitting results for Type A (left) and B (right), regular and irregular models.

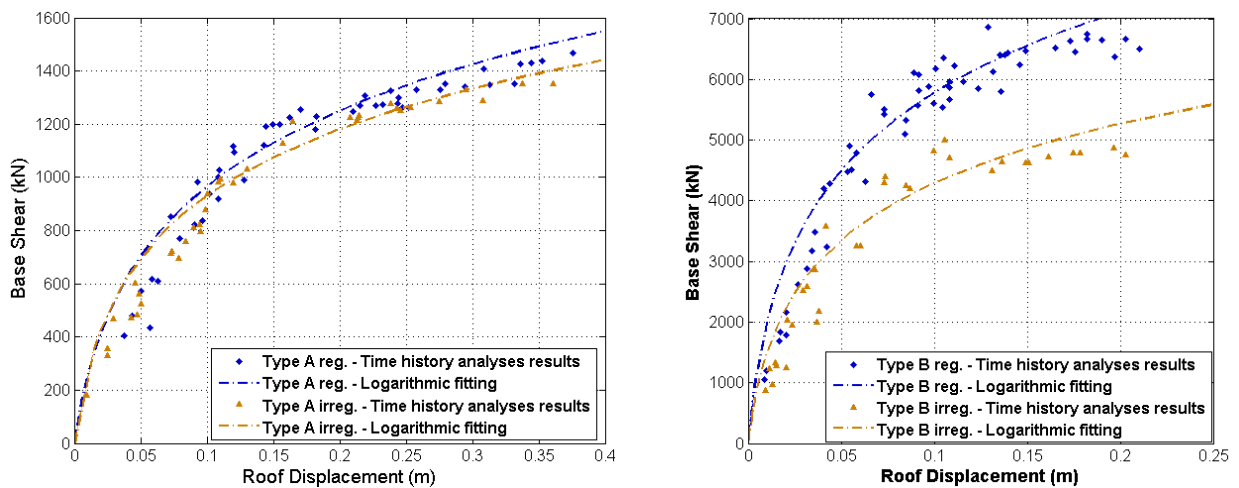


Figure 3.7: Logarithmic fitting results for Type A (left) and B (right), regular and irregular models.

The calculated coefficients (Eq. (3.6; Table 3.3) are based on the results illustrated in Figures



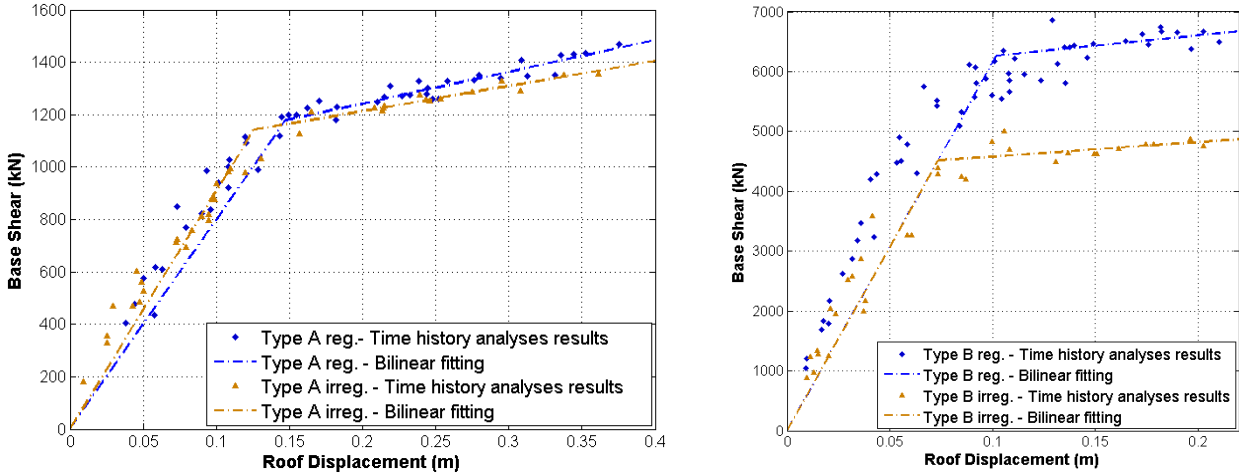


Figure 3.5 Figure 3.6 Figure 3.7. The coefficient values were not very sensitive to the fitting method (less than 8% difference) nor to the global ductility values. The 2<sup>nd</sup> degree polynomial follows best the shape of the pushover curve (Figure 3.1), but cannot provide realistic results for large ductility levels due to the rapid decay of the fitted curve (Figure 3.6). The logarithmic fitting presents quite high initial stiffness and lower base shear at yield (Figure 3.7). Both the logarithmic and the improved bilinear fitting (Chapter 3.1) could be reasonably extrapolated to higher ductility levels for both building-class prototype models (

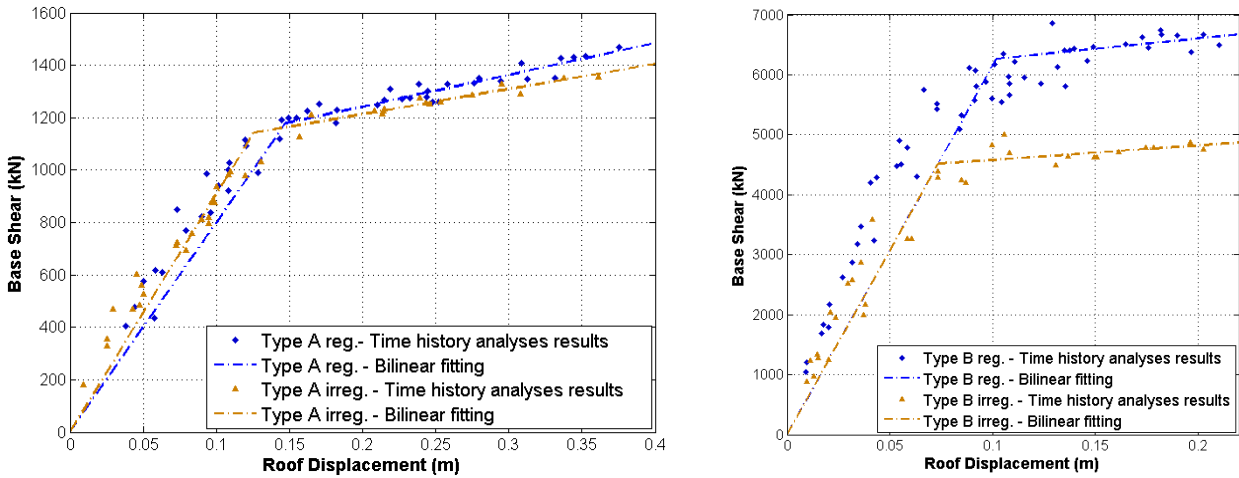


Figure 3.5).

Table 3.3: Coefficients at different ductility levels.

	Type A			Type B		
<i>Fitting curve</i>	Bilinear					
<i>Ductility <math>\mu</math></i>	1	2	3	1	2	3
<i>Coefficient</i>	1.17	1.16	1.17	1.39	1.39	1.38
<i>Fitting curve</i>	2 <sup>nd</sup> degree polynomial					
<i>Ductility <math>\mu</math></i>	1	2	3	1	2	3
<i>Coefficient</i>	1.16	1.15	1.16	1.43	1.30	-



<i>Fitting curve</i>	<i>Logarithmic</i>					
<i>Ductility <math>\mu</math></i>	1	2	3	1	2	3
<i>Coefficient</i>	1.14	1.15	1.15	1.42	1.28	1.43

The selected coefficients will modify the ratio of spectral demand  $S_d(T)\eta$  to building capacity  $\Delta_{capacity}$ , which SP-BELA employs to define whether a specific limit state is exceeded. The coefficients will be applied, with proper interpolation and correlation with damage states, to a percentage of the RC frame building stock in Nablus city, based on the field data collection forms that the locals have filled in the SASPARM 2.0 Web Based Platform and Mobile App, modifying the fragility curves, which for now are representative only of the regular building configurations.

#### 4. CONCLUDING REMARKS

The present report aimed at rendering the aforementioned procedure applicable to a larger population of buildings, thus improving the validity of the implemented methodology. Irregularities in plan and elevation are common in structures that do not comply with any building code; therefore SP-BELA had to be adapted and validated for these cases.

Borzi et al. (2008a, 2008c) have already validated the application of SP-BELA against regular RC frames. For irregular RC frame buildings however, the simplified-pushover based SP-BELA methodology cannot take into account the torsional modes. Two very common irregular RC prototype buildings were examined. The seismic assessment was carried out again through nonlinear time history analyses along the most vulnerable principal direction. The results were used to derive suitable building-class-specific correction factors which will be inserted in the original derivations of SP-BELA, leading to more refined fragility functions.

As noted in deliverable D.F.1, the RC buildings with shear walls have not been tackled through a mechanics-based methodology, since it is not possible to identify a prototype building which can be representative of the whole building stock. Instead, a coefficient has been calibrated to modify the fragility curves of corresponding RC frame configurations. Since the collection forms indicate that the amount of buildings with shear walls is very limited and no prototype building can be attributed to this typology, no further validation has been conducted in the present report.

The masonry buildings in Palestine usually have simple design in plan and no more than two stories. Hence, simplified pushover analyses are representative of the structural performance as long as a global collapse mechanism is activated. In cases of high vulnerable masonry buildings, where local collapse mechanisms govern the performance, SP-BELA has been already calibrated on the bases of observed damage data coming from post-earthquake surveys in Italy (Borzi and Faravelli, 2016). This calibration exercise is considered to be applicable to Nablus, since specific data on post-earthquake surveys are not available in Palestine.



## 5. BIBLIOGRAPHY

Antoniou S and Pinho R. Development and verification of a displacement-based adaptive pushover procedure. *Journal of Earthquake Engineering*, 2004, 8(5): 643-661.

Baker JW. Conditional mean spectrum: Tool for ground-motion selection. *Journal of Structural Engineering*, 2010, 137(3): 322-31.

Bommer JJ, Elnashai AS, Weir AG. Compatible acceleration and displacement spectra for seismic design codes. *12th World Conference on Earthquake Engineering 2000*; Auckland.

Borzi B, Pinho R, Crowley H. Simplified pushover-based vulnerability analysis for large-scale assessment of RC buildings. *Engineering Structures*, 2008, 30(3): 804-820.

Borzi B, Crowley H, Pinho R. Simplified Pushover-Based Earthquake Loss Assessment (SP-BELA) Method for Masonry Buildings. *International Journal of Architectural Heritage*, 2008, 2(4): 353-376.

Borzi B, Crowley H, Pinho R. The Influence of Infill Panels on Vulnerability Curves for RC Buildings. *14th World Conference on Earthquake Engineering 2008*; Beijing, China.

Borzi B, Di Meo A, Faravelli M, Ceresa P, Monteiro R, Dabbeek J. Definition of Fragility Curves for Frame Buildings in Nablus – Palestine. *1st International Conference on Natural Hazards and Infrastructure 2016*; Chania, Greece.

Borzi B, Ceresa P, Franchin P, Noto F, Calvi GM and Pinto PE. Seismic Vulnerability of the Italian Roadway Bridge Stock, *Earthquake Spectra*, 2015, 31(4): 2137-2161.

Borzi B, Faravelli M. Validation of SP-BELA through Comparison with Observed Damage Data, *Engineering Structures* (to be submitted).

Casarotti C, Pinho R. An adaptive capacity spectrum method for assessment of bridges subjected to earthquake action. *Bulletin of Earthquake Engineering*, 2007, 5(3): 377-390.

Chiou BJ, Youngs RR. An NGA model for the average horizontal component of peak ground motion and response spectra. *Earthquake Spectra*, 2008, 24(1): 173-215.

Chopra AK, Goel RK. A modal pushover analysis procedure for estimating seismic demands for buildings. *Earthquake Engineering & Structural Dynamics*, 2002, 31(3): 561-82.

Chopra, AK, Goel RK. Evaluation of the modal pushover analysis procedure for unsymmetric-plan buildings. *1st European Conference on Earthquake Engineering and Seismology*, 2006.

Crisafulli FJ. Seismic behaviour of reinforced concrete structures with masonry infills. *PhD thesis*, 1997; University of Canterbury, New Zealand.

D.B.1: Report on the structural typologies identified during the field investigation and the study of existing projects. *SASPARM 2.0 Deliverable*.

D.B.2: Paper format of the seismic vulnerability forms for citizens and practitioners. *SASPARM 2.0 Deliverable*.



D.B.3: Guidelines for the compilation of seismic vulnerability forms for citizens and practitioners. *SASPARM 2.0 Deliverable*.

D.F.1: Report on the fragility curves for each structural typology that sub-classifies the building stock. *SASPARM 2.0 Deliverable*.

EMME (Earthquake Model of Middle East) Project. Assessment of Seismic Hazard in the Middle East and Caucasus. 2013. [www.emme-gem.org](http://www.emme-gem.org)

Eurocode 2: Design of concrete structures, EN 1992. European Committee for Standardization, 2004; Brussels.

Eurocode 8: Design of Structures for Earthquake Resistance, EN 1998. European Committee for Standardization, 2004, Brussels.

Fajfar P, Gaspersic P. The N2 method for the seismic damage analysis of RC buildings. *Earthquake Engineering and Structural Dynamics*, 1996, 25: 31–46.

Fajfar P. A nonlinear analysis method for performance-based seismic design. *Earthquake Spectra*, 2000, 6: 573–592.

Freeman SA, Nicoletti JP, Tyrell JV. Evaluations of existing buildings for seismic risk — a case study of Puget Sound Naval Shipyard, Bremerton, Washington. *1st US National Conference on Earthquake Engineering*, 1975; Oakland, California.

Grigoratos I, Dabbeek J, Faravelli M, Di Meo A, Cerchiello V, Borzi B, Monteiro R, Ceresa P. Development of A Fragility and Exposure Model for Palestine – Application to the City of Nablus. *World Multidisciplinary Civil Engineering-Architecture-Urban Planning Symposium (WMCAUS)*, 2016; Prague, Czech Republic.

HAZUS 99. Earthquake Loss Estimation Methodology. *Technical Manual*. Federal Emergency Management Agency, 1999; Washington DC.

Jayaram N, Lin T, Baker JW. A computationally efficient ground-motion selection algorithm for matching a target response spectrum mean and variance. *Earthquake Spectra*, 2011, 27(3): 797-815.

Kalkan E, Kunnath SK. Adaptive modal combination procedure for nonlinear static analysis of building structures. *Journal of Structural Engineering*, 2006, 132(11): 1721–1731.

Lawson RS, Vance V, Krawinkler H. Nonlinear Static Push-Over Analysis - Why, When, and How?. *5th U.S. National Conference on Earthquake Engineering*, 1994; Oakland, California.

Masi A. Seismic vulnerability assessment of gravity load designed R/C frames. *Bulletin of Earthquake Engineering*, 2004, 1(3): 371–395.

Monteiro R, Ceresa P, Cerchiello V, Dabbeek J, Di Meo A, Borzi B. Towards integrated seismic risk assessment in Palestine, application to the city of Nablus. *European Congress on Computational Methods in Applied Sciences and Engineering*, 2016; Crete, Greece.

Monteiro R, Marques M, Adhikari G, Casarotti C, Pinho R. Spectral reduction factors evaluation for seismic assessment of frame buildings. *Engineering Structures*, 2014, 77: 129-142.



Pagani M, Monelli D, Weatherill G, Danciu L, Crowley H, Silva V, Simionato M. OpenQuake engine: an open hazard (and risk) software for the global earthquake model. *Seismological Research Letters*, 2014, 85(3): 692-702. [www.globalquakemodel.org/](http://www.globalquakemodel.org/)

Pinho R, Marques M, Monteiro R, Casarotti C, Delgado R. Evaluation of nonlinear static procedures in the assessment of building frames. *Earthquake Spectra*, 2013, 29(4): 1459-1476.

Priestley M. Displacement-based seismic assessment of reinforced concrete buildings. *Journal of Earthquake Engineering*, 1997, 1(1): 157–192.

Priestley M, Calvi GM, Kowalsky M. Displacement-Based Seismic Design of Structures. *IUSS Press*, 2007; Pavia.

Rossetto T, Elnashai A. Derivation of vulnerability functions for European-type RC structures based on observational data. *Engineering Structures*, 2003, 25(10): 1241-1263.

Seismosoft. SeismoStruct v7.0 – A computer program for static and dynamic nonlinear analysis of framed structures. 2014; available from [www.seismosoft.com](http://www.seismosoft.com).

Silva V, Crowley H, Pinho R, Varum H. Extending displacement-based earthquake loss assessment (DBELA) for the computation of fragility curves. *Engineering Structures*, 2013, 56: 343-356.

Silva V, Crowley H, Varum H, Pinho R, Sousa R. Evaluation of analytical methodologies used to derive vulnerability functions. *Earthquake Engineering & Structural Dynamics*, 2014, 43(2): 181-204.

Singhal A, Kiremidjian AS. Method for probabilistic evaluation of seismic structural damage. *Journal of Structural Engineering, ASCE*, 1996, 122(12): 1459–67.

Trifunac, MD, Brady AG. A study on the duration of strong earthquake ground motion. *Bulletin of the Seismological Society of America*, 1975, 65(3): 581-626.

